Analyst

PAPER

View Article Online
View Journal | View Issue

Cite this: *Analyst*, 2015, **140**, 489

Towards improved precision in the quantification of surface-enhanced Raman scattering (SERS) enhancement factors: a renewed approach†

Arumugam Sivanesan,*[ab] Witold Adamkiewicz,[a] Govindasamy Kalaivani,[b] Agnieszka Kamińska,*[a] Jacek Waluk,[a] Robert Hołyst[a] and Emad L. Izake[b]

Received 1st October 2014
Accepted 21st October 2014

DOI: 10.1039/c4an01778a

www.rsc.org/analyst

This paper demonstrates a renewed procedure for the quantification of surface-enhanced Raman scattering (SERS) enhancement factors with improved precision. The principle of this method relies on deducting the resonance Raman scattering (RRS) contribution from surface-enhanced resonance Raman scattering (SERRS) to end up with the surface enhancement (SERS) effect alone. We employed 1,8,15,22-tetraaminophthalocyanato-cobalt(II) (4α-Co^{II}TAPc), a resonance Raman- and electrochemically redox-active chromophore, as a probe molecule for RRS and SERRS experiments. The number of 4α-Co^{II}TAPc molecules contributing to RRS and SERRS phenomena on plasmon inactive glassy carbon (GC) and plasmon active GC/Au surfaces, respectively, has been precisely estimated by cyclic voltammetry experiments. Furthermore, the SERS substrate enhancement factor (SSEF) quantified by our approach is compared with the traditionally employed methods. We also demonstrate that the present approach of SSEF quantification can be applied for any kind of different SERS substrates by choosing an appropriate laser line and probe molecule.

1. Introduction

Surface-enhanced Raman spectroscopy (SERS) was discovered 40 years ago[1] and nowadays it is becoming one of the most popular ultrasensitive analytical techniques.[2,3] Recently, highly sensitive analyses, even at a single molecule level, were achieved with SERS,[4–6] which widened the analytical potential and versatility of this technique. Undoubtedly, the most important issue regarding the SERS effect is the precise quantification of substrate enhancement factors (SSEFs) (*i.e.*, the magnitude of the enhancement). A criticism often underlined is that SERS is still not transferred into practical analytical applications. This is linked with difficulties in measuring the SSEF rigorously. Careful experimental quantification of the SSEF is particularly crucial while designing a useful analytical tool based on SERS. The enhancement factor is also an important figure for characterization of SERS substrates. Although wide varieties of SERS substrates have been produced for the last four decades, there is no standard procedure to assess the quality of the SERS substrate *i.e.*, the issue of precise quantification of the SERS substrate enhancement factor has not been solved until now. The materials chemists involved in the preparation of SERS substrates always face the major problem in sorting out their best substrate. Therefore, also from the materials science point of view, a precise quantification of the SSEF is essential. The questions of the magnitude of the enhancement and the origin of the SERS enhancement are again in the spotlight of researchers, together with those regarding the uncertainty and the interpretation of the pioneering single-molecule (SM) SERS study.[7,8] There are still conflicting viewpoints in SM-SERS, including interpretation of nature and magnitude of the enhancement. Several papers focused on the presentation and discussion of experimental quantification of the enhancement factor.[9–14] However, the reported methods have shortcomings in their approach and methodology. For example, the most widely used equation for the estimation of the SSEF is:[12–14]

$$\mathrm{SSEF} = \frac{I_{\mathrm{SERS}} N_{\mathrm{Vol}}}{I_{\mathrm{RS}} N_{\mathrm{Surf}}} \quad (1)$$

where $N_{\mathrm{Vol}} = c_{\mathrm{RS}} V$ is the average number of molecules in the scattering volume (V) for the Raman (non-SERS) measurement and N_{Surf} is the average number of adsorbed molecules in the scattering volume of the SERS experiments. The above definition presents a few challenges to the accurate quantification of the SERS effect.[15,16]

Arguably, the molecules (Rhodamine 6G, 4-amino-thiophenol, p-mercaptobenzoic acid, *etc.*) which are supposed

[a]*Institute of Physical Chemistry, Polish Academy of Sciences, Kasprzaka 44/52, 01-224 Warsaw, Poland. E-mail: asnesan@gmail.com; sivanesan.arumugam@qut.edu.au; akamin@ichf.edu.pl; Tel: +61 07 3138 0607; +48 22 343 32 28*

[b]*Nanotechnology and Molecular Sciences Discipline, Faculty of Science and Engineering, Queensland University of Technology, 2 George St., Brisbane, QLD 4001, Australia*

† Electronic supplementary information (ESI) available. See DOI: 10.1039/c4an01778a

to be standard objects for the quantification of the SSEF cause difficulty in estimating the Raman cross-section both in solution and also on the surface. Actually, the dye molecules have larger Raman cross-sections up to 10^5–10^6 in resonant[17] and pre-resonant conditions which are not considered in the estimation of the Raman cross-section. In other words, the calculation of the Raman cross-section by density functional theory assumes a non-resonant condition which is suitable for normal Raman spectra. Therefore, the values calculated using this approach will not be applicable even under pre-resonant conditions[18] and hence an alternative approach or method is required. Furthermore, the Raman cross-section may also depend on the effect of the substituents in the probe molecule and also on other factors, that are not considered in the existing quantification equations, such as the interaction with solvent molecules. It is worth mentioning here that I_{Raman} depends on the refractive index of the solvent. Limitations also exist in calculating N_{Surf} as the number of the probe molecules on the surface is estimated by assuming an ideal Langmuir monolayer. In reality, it is hard to achieve a defect-free monolayer. Instead a multilayer of the probe molecule (*e.g.*, 4-aminothiophenol) may exist on the SERS substrate and would result in incorrect estimation of N_{Surf}. Moreover, estimating the surface scattering volume is not rigorous in many cases, as it is difficult to determine the exact active surface area of the substrate. There is also an inconsistency in rigorous quantification of parameters such as effective scattering volume and scattering area in solution. Because these challenges surrounding the optimization and control of experimental parameters in SERS experiments may be one of the reasons for the unusually high SSEF, up to 10^{14}, that are reported in the literature.[16,17]

Recently, Le Ru and coworkers attempted to address these issues by proposing some modifications to eqn (1). These modifications involved introducing several experimental parameters as presented by eqn (2).[16]

$$\mathrm{SSEF} = \frac{I_{\mathrm{SERS}}\left(c_{\mathrm{RS}} H_{\mathrm{eff}}\right)}{I_{\mathrm{RS}}\left(\mu_{\mathrm{M}} \mu_{\mathrm{S}} A_{\mathrm{M}}\right)} \quad (2)$$

here H_{eff} is the effective height of the scattering volume, μ_{M} is the surface density of the individual nanostructures producing the enhancement, μ_{S} is the surface density of the molecules on the surface, and A_{M} represents the surface area of the SERS substrate. Although the above equation is assumed to give rigorous estimation of the SSEF, it is still very hard to experimentally estimate some of the involved parameters with precision. Further, the issue regarding the precise estimation of the Raman cross-section of the probe molecule both in solution and on the surface till persists in this method. Therefore, the aim of this paper is to present a simplified and renewed approach for the experimental quantification of the SSEF with improved precision.

2. Experimental section

2.1. Chemicals and materials

3-Nitrophthalonitrile, cobalt(II) chloride, 1,8-diazabicyclo[5.4.0]-undec-7-ene and hydrogen tetrachloroaurate(III) hydrate were purchased from Sigma-Aldrich. All other chemicals used were of Analytical grade. The chemicals were used without any further purification. Polishing slurries and pads (Microcloth®) were purchased from Buehler, Germany. The diamond polished glassy carbon (GC) discs having a geometric diameter of 0.785 cm^2 (HTW, Germany), polycrystalline gold discs (Au) having a geometric area of 0.502 cm^2 (Mennica Metale Szlachetne, Warsaw, Poland) and indium tin oxide (ITO) coated glass slides (Sigma Aldrich) having a geometric area of 0.250 cm^2 (0.5 × 0.5 cm) were used as working electrodes. A platinum wire (Mennica Metale Szlachetne, Warsaw, Poland) was used as a counter electrode. A dry leakless electrode (DRIREF-2, World Precision Instruments, USA) was used as a reference electrode.

2.2. Instrumentation

All electrochemical experiments were carried out using a μAutolab potentiostat (Metrohm Autolab) with a custom-made three-electrode cell setup. All Raman measurements were performed using the Renishaw InVia Raman system equipped with 785 nm and 514 nm laser lines as excitation sources. The laser light was passed through a line filter and focused on a sample mounted on an *X*–*Y*–*Z* translation stage with a 50× objective lens (numerical aperture 0.55) that focused the laser to a spot size of around 5 μm. The Raman-scattered light was collected by the same objective through a holographic notch filter to block the Rayleigh scattering. A 1800 groove per mm grating (514 nm source) and a 1200 groove per mm grating (785 nm source) were used to provide a spectral resolution of 5 cm^{-1}. The Raman scattering signal was recorded using a 1024 × 256 pixel RenCam CCD detector. Typically, the spectra were acquired for 4 s, with the laser power measured at the sample ranging from 1 mW to 50 mW. SERS mapping was performed over all the substrates investigated and each spectrum presented here is the average of 50 spectra. SEM measurements were performed using a FEI Nova™ NanoSEM Scanning Electron Microscope 450 with an accelerating voltage of 2 kV under high vacuum.

2.3. Synthesis of 1,8,15,22-Tetraaminophthalocyanatocobalt(II)

1,8,15,22-Tetraaminophthalocyanatocobalt(II) (4α-Co^{II}TAPc) (Scheme S1†) was synthesized based on the reported procedure.[19,20] 3-Nitrophthalonitrile (2.0 g, 11.6 mmol), cobalt(II) chloride (0.83 g, 3.5 mmol) and a catalytic amount of 1,8-diazabicyclo[5.4.0]-undec-7-ene (DBU) were mixed together in a refluxing flask along with 100 mL of *n*-pentanol and refluxed for 12 h. The product was washed and centrifuged with methanol–water solution (v/v, 1/1) 3 times to get pure 1,8,15,22-tetranitrophthalocyanatocobalt(II). Then it was suspended in water (150 mL) along with sodium sulfide (8 g) and stirred for 7 h at 50 °C. The solid product obtained after filtration was washed with dilute HCl and water. The product was again washed with water and methanol each 3 times and dried.

2.4. SERS substrate preparation

GC and Au disc electrodes were mechanically mirror-polished with alumina slurries with sequentially decreasing particle sizes (0.5 μm, 0.05 μm and 0.02 μm). After each step of polishing, the

electrodes were immersed in Millipore water and subsequently sonicated in an aqueous ultrasonic bath for 15 minutes to remove the physically adsorbed alumina particles from the electrode surface. The ITO coated glass slides were cleaned by sonicating in acetone followed by ethanol for 15 minutes each. All the electrodes were finally washed with Millipore water and dried with a flow of argon gas.

The nanostructured SERS substrate was prepared by potentiostatic deposition of gold over GC (GC/Au), Au (pAu/Au) and ITO (ITO/Au). The three-electrode electrochemical cell was filled with the solution of 4 mM $HAuCl_4$ in 0.1 M $HClO_4$ and subsequently purged with argon gas for 30 min to remove most of the air from the solution. A potential of −80 mV was applied for 400 s and then the electrode was removed from the solution and subsequently washed with Millipore water to remove other ions from the surface. The electrode was then dried with flow of argon gas and used as a SERS substrate.

2.5. Self-assembly of tetraaminophthalocyanatocobalt(II) on Au surfaces

The real surface area of GC/Au, pAu, pAu/Au, and ITO/Au was estimated from the charge required to reduce the surface gold oxide layer.[21] The geometric area of the GC (10 mm) and Au (8 mm) electrodes was calculated using the diameter of the employed electrodes. The ratio of the real surface area to the geometric area represents the surface roughness factor. The self-assembled monomolecular film (SAM) of 4α-Co^{II}TAPc was formed by soaking the cleaned GC and GC/Au electrode in 1 mM DMF solution of 4α-Co^{II}TAPc overnight. The electrode was then removed from the solution and repeatedly washed with DMF and then dipped in DMF for 30 min to remove physically adsorbed molecules from the electrode surface and finally washed with water. The charge under the anodic wave corresponding to the oxidation of Co(II) was used to calculate the surface coverage (Γ). Fig. S1† shows the UV-visible spectrum of 4α-Co^{II}TAPc SAM on the ITO surface.

2.6. RRS and SERRS experiments

In order to reduce the error in quantification of the SSEF, the same substrates were used for RRS/SERRS and cyclic voltammetry experiments. In addition, RRS/SERRS experiments were performed first then followed by cyclic voltammetry so that the effect of electrochemical reaction on the orientation of the molecule and hence the Raman signal is excluded.

3. Results and discussion

3.1. Overview of the renewed approach

Previously, Hildebrandt and Stockburger demonstrated an approach and a mathematical equation for the quantification of the SSEF.[22] We recently employed the equation given by Hildebrandt *et al.*[22] for the quantification of the SSEF for silver colloids.[22–25] The modified form of that equation is:

$$\mathrm{SSEF} = \frac{I_{\mathrm{SERRS}} c_{\mathrm{RRS}}}{I_{\mathrm{RRS}} c_{\mathrm{SERRS}}} \quad (3)$$

here, c_{RRS} and c_{SERRS} are the concentrations of molecules involved in resonance Raman scattering (RRS) and surface-enhanced resonance Raman scattering (SERRS), respectively. The parameter shielding constant (k) is removed from the original equation.[22] Since the SERRS experiments in the present work have been carried out on the solid substrate with a monolayer of the probe molecule, the possibility of shielding effect contribution is negligible.

The principle of our approach to estimate the SSEF is based on deducting the RRS effect from SERRS. To achieve this demonstrating both RRS and SERRS in solid surfaces modified with a monolayer of the electro- and Raman-active probe molecule is very crucial. In addition, for the success of this approach, all important parameters such as Raman cross-section, focal volume and laser power must remain the same in both the RRS and SERRS experiments. By measuring both the RRS (plasmon inactive) and SERRS (plasmon active) on surfaces having a monolayer of electro- and Raman-active probe molecules, we can avoid the quantification of parameters such as focal volume, solvent effect, shielding effect and inner filter effect. The compound which satisfies our needs to quantify the SSEF based on the renewed approach is 1,8,15,22-tetraaminophthalocyanatocobalt(II) (4α-Co^{II}TAPc). It forms a very stable monomolecular film on GC,[26] Au,[27,28] Ag[27] and indium tin oxide (ITO)[29] surfaces. 4α-Co^{II}TAPc is a very good electro-active molecule which demonstrates a well-defined redox peak for the Co^{II}/Co^{III} redox couple.[19,28] In addition, 4α-Co^{II}TAPc shows a very strong absorption band, known as Q band, around 750 nm in UV-visible spectroscopy.[29]

Now comes the issue of the Raman cross-section, a critical point which has to be addressed. In fact, the key assumption in the present approach is that, identifying the Raman cross-section of the probe molecule is not necessary (see Section 4 for details) since in both the RRS and SERRS experiments, the chromophore (4α-Co^{II}TAPc) is under resonant conditions. However, estimating the parameters c_{RRS} and c_{SERRS} in eqn (3) remains a challenge. Currently in all the existing methods, c_{RRS} and c_{SERRS} cannot be accurately measured without making some theoretical assumptions.[14,16] Nevertheless, based on our renewed approach, the above two parameters can be rigorously quantified by preparing a self-assembled monolayer (SAM) of an electrochemically redox-active chromophore molecule. In the present method, we developed a monolayer of 4α-Co^{II}TAPc on plasmon inactive glassy carbon (GC) and plasmon active nanostructure gold over GC (GC/Au) surfaces/electrodes such that both the surfaces are suitable for electrochemical and Raman (RRS and SERRS) experiments. By integrating the charge under the redox wave of the cyclic voltammograms obtained for 4α-Co^{II}TAPc, the surface coverage *i.e.*, c_{RRS} and c_{SERRS} can be accurately estimated (*vide infra*). Now, eqn (3) can be rearranged as:

$$\mathrm{SSEF} = \frac{I_{\mathrm{SERRS}} \Gamma_{\mathrm{RRS}}}{I_{\mathrm{RRS}} \Gamma_{\mathrm{SERRS}}} \quad (4)$$

where, Γ_{RRS} and Γ_{SERRS} are the surface coverage of the probe molecule on GC and GC/Au surfaces, respectively. Here on the GC surface, selecting an excitation laser line which is in

resonance with the chromophore leads to RRS enhancement only since the SERS effect is completely excluded on the GC surface. On the other hand, on the GC/Au surface, the chromophore experiences both RRS and SERRS phenomena. Since the exact surface coverage of 4α-Co^{II}TAPc on both RRS and SERRS active surfaces are known and also other parameters such as laser power, focal area and Raman cross-section remain the same for both the experiments, eqn (4) is expected to provide a SSEF value with improved accuracy than the previous methods.

We elected the compound 1,8,15,22-tetraaminophthalocyanatocobalt(II) (4α-Co^{II}TAPc) as it satisfies the sought criteria for the chromophore in our experiments. It is a very good redox-active molecule with a strong absorption band around 750 nm (Scheme S1†). Moreover, it forms a stable monomolecular film on GC, Au, Ag and indium tin oxide (ITO).[26,28,29]

3.2. Preparation, characterization and estimation of the real surface area of the SERS substrates

The SERS substrate used in the present investigation was prepared by potentiostatic deposition of nanostructured Au over the mirror polished GC surface/electrode. Here Au has been preferred over the traditionally used silver surface due to several reasons such as: (i) the wide potential window of Au which makes the surface appropriate for the 4α-Co^{II}TAPc redox couple, (ii) the ability to precisely estimate the real surface by electrochemical methods, (iii) the plasmonic band of nanostructured Au is red-shifted in contrast to rough silver, which will result in an increased SERS effect with a red excitation line, and (iv) stability of the Au surface in open air. The surface morphology of the GC/Au substrate was characterized by scanning electron microscopy (SEM) experiments (Fig. 1). The SEM picture clearly reveals a defect-free uniform deposition of Au nanostructures in the size ranging from 10 to 100 nm. The ellipsometry experiment depicts that the absorption maximum of the GC/Au substrate is around 500 nm (Fig. S2†).

It is well-established in the literature[21,30] that the real surface area of gold could be achieved electrochemically by integrating the charge under the gold oxide reduction peak. In the present study, a similar electrochemical approach has been followed to quantify the real surface area of the GC/Au SERRS substrate.[24,25] Further, we used diamond polished GC surfaces in all our experiments since they have the very flat surface with negligible surface roughness. Therefore, in the case of diamond polished GC, the geometric area and real surface area are almost similar. However, it is important to note that the real surface of the SERS-active substrate is not equivalent to its geometric surface since a SERS-active substrate is always highly roughened. In most of the previous SSEF calculation methods, the difference between the real and geometric areas was not clearly accounted.

The real surface area of Au nanostructure over the GC surface has been precisely quantified through cyclic voltammetry (Fig. S3†).[21] By integrating the charge under the gold oxide reduction peak, the real surface of Au was found to be 3.02 cm^2 which is 3.98 times higher than the geometric surface area (0.785 cm^2).[21] As diamond polished GC is known for its highly polished surface, the surface roughness is almost negligible in the case of the GC surface.

3.3. Estimation of surface coverage of 4α-Co^{II}TAPc on both GC and GC/Au surfaces

The ability of 4α-Co^{II}TAPc to form the monomolecular film on GC and GC/Au surfaces, *via* chemisorptions, and subsequent precise quantification of its surface coverage by the cyclic voltammetry method is well documented in the literature.[26,28,29] Since the real surface area of both the surfaces (GC and GC/Au) has now been identified (see Section 3.2), the surface coverage of the 4α-Co^{II}TAPc monomolecular film on GC (Γ_{RRS}) and GC/Au (Γ_{SERRS}) surfaces can also be quantified by integrating the charge under redox waves of the obtained cyclic voltammogram shown in Fig. 2. The cyclic voltammograms (CVs) of GC/4α-Co^{II}TAPc and GC/Au/4α-Co^{II}TAPc electrodes were obtained in 0.1 H_2SO_4 (Fig. 2). The CVs showed a pair of well-defined redox couple with an $E_{1/2}$ value around 0.34 V corresponding to the Co^{III}/Co^{II} redox couple.[19,26] The surface coverage (Γ) of 4α-Co^{II}TAPc SAM on GC and on GC/Au electrodes has been estimated by

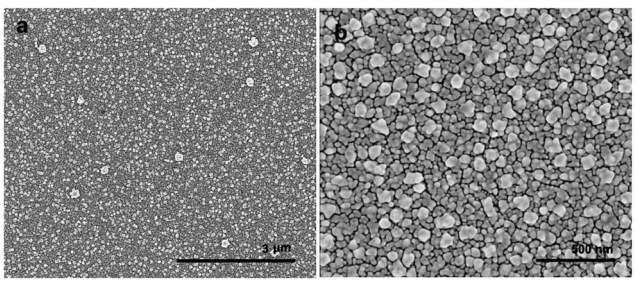

Fig. 1 SEM images of nanostructured Au electrodeposited over mirror polished GC.

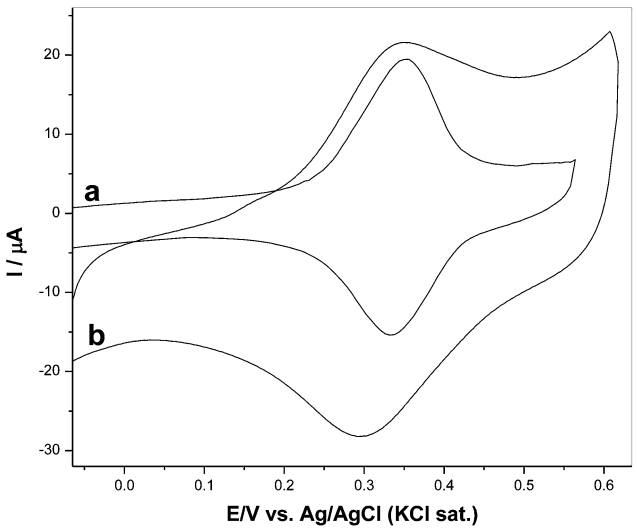

Fig. 2 Cyclic voltammograms obtained for self-assembled monomolecular films of 4α-Co^{II}TAPc on (a) GC and (b) GC/Au electrodes in 0.1 M H_2SO_4 at a scan rate of 0.1 V s^{-1}.

integrating the charge under the anodic wave (Co^{II} oxidation) of the cyclic voltammogram. The Γ values of 2.25×10^{-10} mol cm^{-2} and 8.61×10^{-11} mol cm^{-2} have been estimated for 4α-Co^{II}TAPc SAM on GC and on GC/Au surfaces/electrodes, respectively. The values are in good agreement with the reported values.[26] The increased surface coverage on the glassy carbon electrode is attributed in part to the additional π-stacking effect of 4α-Co^{II}TAPc on the glassy carbon surface.[26] On the other hand, contribution of π-stacking on the gold surface is insignificant.

3.4. Quantification of the SERS substrate enhancement factor (SSEF)

Fig. 3 shows the RRS and SERRS spectra of 4α-Co^{II}TAPc SAM on GC and GC/Au surfaces, respectively. Both RRS and SERRS spectra on all surfaces showed two intense bands at 1551 cm^{-1} and 756 cm^{-1} corresponding to macrocycle in-plane stretching and macrocycle deformation, respectively.[27,31,32] Moreover, the RRS spectrum on the GC surface showed two intense bands at 1309 cm^{-1} and 1606 cm^{-1} corresponding to the stretching and breathing modes of sp^2 hybridized carbon.[33] To quantify the SSEF, the band at 756 cm^{-1} is used as a reference. Based on eqn (4), the SSEF of the GC/Au surface has been calculated and it was found to be $(2.82 \pm 0.22) \times 10^4$. It is worth mentioning at this juncture that all the 50 SERRS spectra recorded at different spots on the GC/Au surface have a similar intensity ratio among the different stretching bands confirming that all the 4α-Co^{II}TAPc molecules adopt same orientation over the entire substrate. We have also carried out the Raman experiment of 4α-Co^{II}TAPc SAM on the GC surface under non-resonance conditions using a 514 nm laser line as the excitation source. The absence of Raman bands corresponding to the 4α-Co^{II}TAPc molecule even after increasing the laser accumulation to 10 times higher than that used for the RRS measurement with a 785 nm laser line confirms that there is no charge-transfer enhancement on the GC surface. This clearly implies that only resonance Raman effect contributes to the Raman spectrum of 4α-Co^{II}TAPc SAM on the GC surface under red light excitation (785 nm). Further, it is worth mentioning here that the overall estimated SSEF by the present method is the average value from the whole surface and not at a particular spot. Therefore, the quantified SSEF by the present method is the average SSEF (ASSEF).

3.5. Quantification of the SSEF of ITO/Au and pAu/Au substrates

In order to confirm the present approach could be used for a wide variety of surfaces, we have performed the same experiment on Au deposited on indium tin oxide (ITO/Au) and also on the Au deposited over mirror polished Au surface (pAu/Au). Fig. 4 shows the SEM pictures of ITO/Au and pAu/Au substrates and it clearly depicts that the Au nanostructures are uniformly deposited over the entire surface. Further, a closer look reveals that the size of Au nanostructures deposited over the polished Au surface is smaller than those deposited over GC and ITO surfaces. The probable cause may be the particle initiation spots on the Au surface that are higher than the other surfaces due to a better Au–Au interaction. Similar to the GC/Au surface, the real surface area of nanostructured pAu/Au and ITO/Au was estimated from the gold oxide reduction peak (Fig. S4†) and it was found to be 2.33 cm^2 and 4.84 cm^2, respectively. The Γ values of 4.96×10^{-11} mol cm^{-2} and 1.27×10^{-11} mol cm^{-2} have been estimated for 4α-Co^{II}TAPc SAM on pAu/Au and ITO/Au surfaces/electrodes, respectively (Fig. S5†).

For the estimation of the SSEF in all the three SERS substrates, RRS of 4α-Co^{II}TAPc performed on the GC surface has been used as a common reference since one can be certain

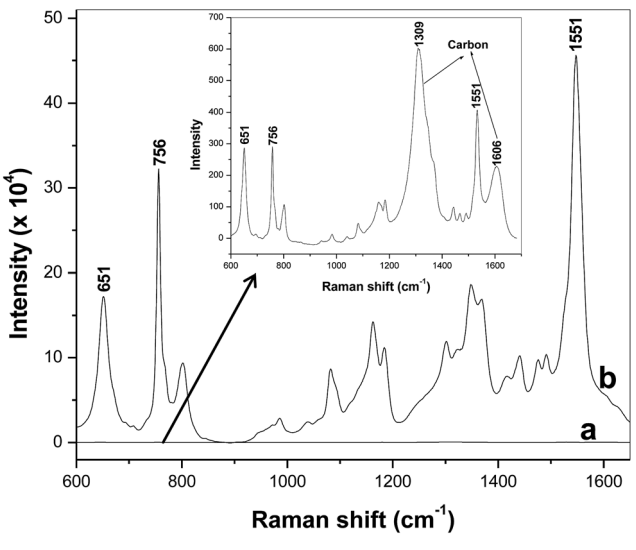

Fig. 3 (a) RRS and (b) SERRS spectra of the self-assembled monomolecular film of 4α-Co^{II}TAPc on GC and GC/Au surfaces. The inset shows the closer view of the RRS spectrum.

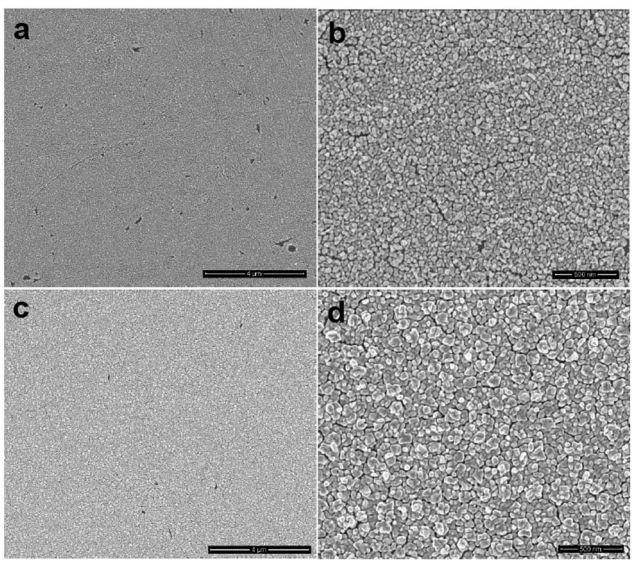

Fig. 4 SEM images of nanostructured Au electrodeposited over polished Au (a and b) and ITO (c and d) substrates captured at different magnifications.

that GC is a plasmon-inactive surface and therefore it will not provide SERS enhancement. Fig. 5 shows the SERS spectra of 4α-Co^{II}TAPc on pAu/Au and ITO/Au substrates. The SSEF of ITO/Au and pAu/Au was quantified by substituting the above values in eqn (4) and it was found to be $(6.3 \pm 0.59) \times 10^4$ and $(2.1 \pm 0.19) \times 10^5$, respectively (nearly 1 order higher SSEF on pAu/Au than other two substrates). This may be attributed to the possible coupling between the propagating surface plasmon polariton (SPP) of the underlying polished Au surface and surface plasmon resonance (SPR) of the Au nanostructures *i.e.*, SPP–SPR coupling.[34] In addition, the nanostructures on pAu has a smaller grain size than on GC or ITO surfaces which allow the possibility for more 'hot spots' in the former surface and subsequent higher SSEF.

3.6. Analyzing the SSEF values of the present method with the traditional method

To have a comparative study, we have calculated the SSEF for our substrates in the traditional way of calculation *i.e.*, using the parameters N_{Vol} and N_{Surf}. The number of molecules in the surface, N_{Surf}, is calculated by assuming a Langmuir monolayer.

As we discussed previously, it is hard to accurately estimate the number of molecules in the solution medium that exists under the focus of the laser beam. To have a better comparison, we considered three possible focal volumes such as cylindrical, fusiform and whole cell length for the estimation of N_{Vol}. Table 1 indicates the SSEF values acquired using our method in comparison to those obtained by the traditional method.[14,16] It can be observed from the table that the SSEF values calculated by the traditional method show significantly greater variations than those calculated using eqn (4). These results indicate the improved precession in our approach when compared to the traditional approach.

4. Addressing critical issues

In spite of all the above explanations of the renewed approach, there are few issues and shortcomings in the above equation which have to be criticized and addressed. In our approach, the RRS effect of 4α-Co^{II}TAPc is assumed to be similar on both GC and GC/Au surfaces. This assumption may not be completely valid since there will be some differences between the two surfaces with respect to the RRS effect. This is due to the potential differences in the surface binding nature of the 4α-Co^{II}TAPc molecules on each surface. Actually, RRS effect is directly related to the Raman cross-section and since the present study involved the RRS and SERRS measurements on surfaces having a monomolecular 4α-Co^{II}TAPc film, the Raman cross-section exclusively depends on the charge-transfer effect *i.e.* the chemical enhancement factor (CHEF). In other words, the difference in surface binding nature of 4α-Co^{II}TAPc on GC and GC/Au surfaces, more precisely the difference in the chemical enhancement factor (CHEF), is playing a key role in our assumption rather than the molecular orientation of the chromophore on the surface. It is well-known that the contribution of the chemical enhancement factor (CHEF) to the overall SSEF is small even for organothiols on noble metal nanoparticles.[11] Considering the fact that the binding affinity of amino groups on GC or Au is comparatively weaker than the binding affinity of thiols on the gold surface, the contribution of the CHEF in the present study is assumed to be even less than the values indicated in the literature for organothiol-noble metal interactions.[11] Overall, in the present method, it is only the ratio between the CHEF of chromophore on the GC and GC/Au surfaces contributing to the overall SSEF and we believe that this will be an insignificant number. Further, a recent report[35] demonstrated that the chemical effect hardly influences the resonance Raman effect in particular for larger molecules such as Rhodamine 6G which further supports our assumption. Therefore, we believe that the difference in the RRS effect *i.e.*, charge-transfer effect of 4α-Co^{II}TAPc on both surfaces is negligible.

The other major concern for the readers would be the feasibility of the present approach to quantify the SSEF for the non-conducting surface. In principle, the methodology could be extended to non-conductive surfaces. The real surface area of any nanostructure surface could be precisely estimated by the Brunauer–Emmett–Teller (BET) gas adsorption method[36] and subsequently one can relatively estimate the number of 4α-Co^{II}TAPc on any Au nanostructured surface by using the standard surface coverage value of 4α-Co^{II}TAPc on the Au surface (8.61×10^{-11} mol cm^{-2}) estimated electrochemically.[28] Since

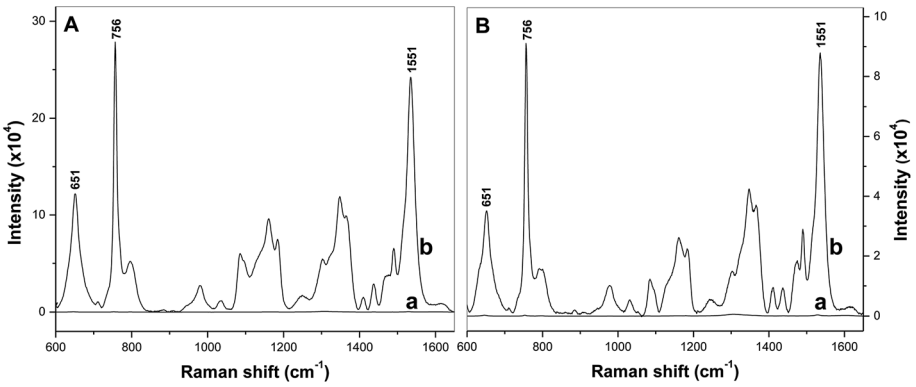

Fig. 5 SERRS spectra of the self-assembled monomolecular film of 4α-Co^{II}TAPc on pAu/Au (Ab) and ITO/Au (Bb) substrates. RRS spectrum of the self-assembled monomolecular film of 4α-Co^{II}TAPc on GC (both Aa and Ba) which is the replicate of Fig. 3 (inset).

Table 1 Comparison of the SSEF of the all the three substrates calculated by the present approach with the traditional method

	Traditional way of SSEF calculation			
SERS substrate	Cylindrical laser beam	Fusiform laser beam	Whole cell length	Present method
GC/Au	4.9×10^3	1.6×10^3	1.1×10^6	2.8×10^4
pAu/Au	2.1×10^4	6.9×10^3	4.6×10^6	2.1×10^5
ITO/Au	7.2×10^3	2.4×10^3	1.6×10^6	6.3×10^4

surface coverage of 4α-Co^{II}TAPc is directly related to the gold surface area irrespective of the surface morphology of the gold surface, we strongly believe that the above value (8.61×10^{-11} mol cm^{-2}) is valid for any gold surface. As evidence, the present number is already going in hand with the literature.[28] Thus, by assessing the RRS and SERRS intensity of 4α-Co^{II}TAPc, respectively on diamond polished GC and SERRS active Au surfaces along with the real surface area (BET method) of the SERRS active Au substrate, one can relatively quantify the SSEF of a new Au surface by utilizing the surface coverage value of 4α-Co^{II}TAPc on GC and GC/Au surfaces from the present work as a standard value.

The equation proposed in our study (eqn (4)), in the present form, may not be suitable to quantify the SSEF from colloidal nanoparticles. This is because several other parameters must be included in the equation. For example, the precise surface area of the nanoparticles, the surface coverage by the probe molecule, contribution of EF from second and subsequent layers of the analyte on the nanoparticle surface, the shielding and inner filter effect of the nanoparticles will be required for the quantification of the SSEF.

5. Conclusions

In summary, we have derived a most simplified equation, of improved precision, for the quantification of the SSEF by a renewed approach. This approach uses electroactive and SERRS active 4α-Co^{II}TAPc as a probe molecule. The SSEF from the GC/Au, pAu/Au and ITO/Au SERS substrates has been quantified using 4α-Co^{II}TAPc as a standard molecule for red light excitation. The number of 4α-Co^{II}TAPc molecules involved in RRS and SERRS has been precisely quantified by electrochemical experiments.

Our approach relies on performing RRS on the Plasmon-inactive conductive surface and subsequently deducting RRS from SERRS to end up with surface enhancement. This approach is also based on the assumption that the resonance enhancement in the Raman spectra is surface-independent. It is important to note that the SSEF of a substrate is related to the excitation laser used since each surface has its own surface plasmon resonance frequency. Thus, the calculated SSEF for all three substrates is applicable only for the 785 nm laser line. The present approach for SSEF quantification can be extended to the quantification of the SSEF from various conducting and non-conducting SERS substrates at various excitation wavelengths provided redox-active Raman chromophores suitable for each laser line. We are presently working towards the quantification of the SSEF from the silver surface using a substituted porphyrin and also the BET method to estimate the real surface area. This chromophore is electroactive and resonance Raman active at 413 nm excitation line, and therefore, satisfies the requirements of our proposed approach.

Acknowledgements

The research was supported by the Foundation for Polish Science – POMOST Programme co-financed by the European Union within European Regional Development Fund. AS was supported by the EC 7.FP under the Research Potential (Coordination and Support Actions FP7-REGPOT-CT-2011-285949-NOBLESSE). W.A. was supported by the Polish National Center of Research and Development in the project from the funds granted on the basis of the decision number: PBS2/A1/8/2013. R.H. was supported by the National Science Center in the project from the funds granted on the basis of the decision number: DEC-2013/08/W/NZ1/00687 (SYMFONIA). AS sincerely thanks Prof. Godwin Ayoko, Dr Bill Lott, Prof. Peter Fredericks, Prof. Esa Jaatinen and Dr Llew Rintoul from QUT for their valuable discussion and support.

References

1 M. Fleischmann, P. Hendra and A. McQuillan, *Chem. Phys. Lett.*, 1974, **26**, 163–166.
2 A. Sivanesan, E. Witkowska, W. Adamkiewicz, Ł. Dziewit, A. Kamińska and J. Waluk, *Analyst*, 2014, **139**, 1037–1043.
3 S.-C. Luo, K. Sivashanmugan, J.-D. Liao, C.-K. Yao and H.-C. Peng, *Biosens. Bioelectron.*, 2014, **61**, 232–240.
4 S. S. R. Dasary, A. K. Singh, D. Senapati, H. Yu and P. C. Ray, *J. Am. Chem. Soc.*, 2009, **131**, 13806–13812.
5 W. Ren, Y. Fang and E. Wang, *ACS Nano*, 2011, **5**, 6425–6433.
6 E.-Z. Tan, P.-G. Yin, T.-t. You, H. Wang and L. Guo, *ACS Appl. Mater. Interfaces*, 2012, **4**, 3432–3437.
7 S. Nie and S. R. Emory, *Science*, 1997, **275**, 1102–1106.
8 K. Kneipp, Y. Wang, H. Kneipp, L. T. Perelman, I. Itzkan, R. R. Dasari and M. S. Feld, *Phys. Rev. Lett.*, 1997, **78**, 1667.
9 M. Muniz-Miranda and G. Sbrana, *J. Phys. Chem. B*, 1999, **103**, 10639–10643.
10 S. M. Ansar, X. Li, S. Zou and D. Zhang, *J. Phys. Chem. Lett.*, 2012, **3**, 560–565.

11 F. S. Ameer, W. Hu, S. M. Ansar, K. Siriwardana, W. E. Collier, S. Zou and D. Zhang, *J. Phys. Chem. C*, 2013, **117**, 3483–3488.
12 W. B. Cai, B. Ren, X. Q. Li, C. X. She, F. M. Liu, X. W. Cai and Z. Q. Tian, *Surf. Sci.*, 1998, **406**, 9–22.
13 A. D. McFarland, M. A. Young, J. A. Dieringer and R. P. Van Duyne, *J. Phys. Chem. B*, 2005, **109**, 11279–11285.
14 E. C. Le Ru and P. G. Etchegoin, *MRS Bull.*, 2013, **38**, 631–640.
15 M. J. Natan, *Faraday Discuss.*, 2006, **132**, 321–328.
16 E. C. Le Ru, E. Blackie, M. Meyer and P. G. Etchegoin, *J. Phys. Chem. C*, 2007, **111**, 13794–13803.
17 L. Jensen and G. C. Schatz, *J. Phys. Chem. A*, 2006, **110**, 5973–5977.
18 S. A. Meyer, E. C. L. Ru and P. G. Etchegoin, *J. Phys. Chem. A*, 2010, **114**, 5515–5519.
19 A. Sivanesan and S. Abraham John, *Electrochim. Acta*, 2008, **53**, 6629–6635.
20 A. Sivanesan and S. A. John, *Biosens. Bioelectron.*, 2007, **23**, 708–713.
21 J. C. Hoogvliet, M. Dijksma, B. Kamp and W. P. Van Bennekom, *Anal. Chem.*, 2000, **72**, 2016–2021.
22 P. Hildebrandt and M. Stockburger, *J. Phys. Chem.*, 1984, **88**, 5935–5944.
23 A. Sivanesan, H. K. Ly, J. Kozuch, M. Sezer, U. Kuhlmann, A. Fischer and I. M. Weidinger, *Chem. Commun.*, 2011, **47**, 3553–3555.
24 G. Kalaivani, A. Sivanesan, A. Kannan, N. S. Venkata Narayanan, A. Kaminska and R. Sevvel, *Langmuir*, 2012, **28**, 14357–14363.
25 A. Sivanesan, J. Kozuch, H. K. Ly, G. Kalaivani, A. Fischer and I. M. Weidinger, *RSC Adv.*, 2012, **2**, 805–808.
26 A. Sivanesan and S. A. John, *Electrochim. Acta*, 2009, **54**, 7458–7463.
27 M. P. Somashekarappa and S. Sampath, *Chem. Commun.*, 2002, 1262–1263.
28 A. Sivanesan and S. Abraham John, *Langmuir*, 2008, **24**, 2186–2190.
29 A. Sivanesan and S. Abraham John, *J. Electroanal. Chem.*, 2009, **634**, 64–67.
30 S. Trasatti and O. A. Petrii, *J. Electroanal. Chem.*, 1992, **327**, 353–376.
31 C. Jennings, R. Aroca, A.-M. Hor and R. O. Loutfy, *J. Raman Spectrosc.*, 1984, **15**, 34–37.
32 X. Li, W. Xu, X. Wang, H. Jia, B. Zhao, B. Li and Y. Ozaki, *Thin Solid Films*, 2004, **457**, 372–380.
33 D. R. Tallant, J. E. Parmeter, M. P. Siegal and R. L. Simpson, *Diamond Relat. Mater.*, 1995, **4**, 191–199.
34 N. Félidj, J. Aubard, G. Lévi, J. R. Krenn, G. Schider, A. Leitner and F. R. Aussenegg, *Phys. Rev. B: Condens. Matter Mater. Phys.*, 2002, **66**, 245407.
35 K.-i. Yoshida, T. Itoh, H. Tamaru, V. Biju, M. Ishikawa and Y. Ozaki, *Phys. Rev. B: Condens. Matter Mater. Phys.*, 2010, **81**, 115406.
36 Y. H. Tan, J. A. Davis, K. Fujikawa, N. V. Ganesh, A. V. Demchenko and K. J. Stine, *J. Mater. Chem.*, 2012, **22**, 6733–6745.